ESB Clinical Biomechanics Award 2020: Pelvis and hip movement strategies discriminate typical and pathological femoral growth – Insights gained from a multi-scale mechanobiological modelling framework

Author

Kainz, H, Killen, BA, Van Campenhout, A, Desloovere, K, Garcia Aznar, JM, Shefelbine, S, Jonkers, I

Published

2021

Journal Title

Clinical Biomechanics

Version

Version of Record (VoR)

DOI

10.1016/j.clinbiomech.2021.105405

Clinical Biomechanics 87 (2021) 105405

Contents lists available at ScienceDirect

Clinical Biomechanics

journal homepage: www.elsevier.com/locate/clinbiomech

Original articles

ESB Clinical Biomechanics Award 2020: Pelvis and hip movement strategies discriminate typical and pathological femoral growth – Insights gained from a multi-scale mechanobiological modelling framework

Hans Kainz [a,*], Bryce A. Killen [b], Anja Van Campenhout [c,d,e], Kaat Desloovere [c,f], Jose Manuel Garcia Aznar [g], Sandra Shefelbine [h], Ilse Jonkers [b]

[a] Centre for Sport Science and University Sports, Department of Biomechanics, Kinesiology and Computer Science in Sport, University of Vienna, Austria,
[b] Human Movement Biomechanics Research Group, KU Leuven, Belgium
[c] Clinical Motion Analysis Laboratory, University Hospital Leuven, Leuven, Belgium
[d] Department of Development and Regeneration, KU Leuven, Leuven, Belgium
[e] Department of Orthopaedics, University Hospital Leuven, Leuven, Belgium
[f] Department of Rehabilitation Sciences, KU Leuven, Belgium
[g] Department of Mechanical Engineering, University of Zaragoza, Spain
[h] Department of Bioengineering, Northeastern University, Boston, USA

A B S T R A C T

Background: Many children with cerebral palsy (CP) develop skeletal deformities during childhood. So far, it is unknown why some children with CP develop bony deformities whereas others do not. The aims of this study were to (i) investigate what loading characteristics lead to typical and pathological femoral growth, and (ii) evaluate why some children with CP develop femoral deformities whereas other do not.
Methods: A multi-scale mechanobiological modelling workflow was used to simulate femoral growth based on three-dimensional motion capture data of six typically developing children and 16 children with CP. Based on the growth results, the participants with CP were divided into two groups: typical growth group and pathological growth group. Gait kinematics and femoral loading were compared between simulations resulting in typical growth and those resulting in pathologic growth.
Findings: Hip joint contact forces were less posteriorly-oriented in the pathological growth simulations compared to the typical ones. Compared to the typically developing participants, the CP group with pathological femoral growth presented increased knee flexion and no hip extension. The CP group with simulated typical growth presented similar sagittal plane joint kinematics but differed in the frontal plane pelvic and hip movement strategy, which normalized the hip joint contact force and therefore contributed to typical femoral growth trends.
Interpretation: Our simulation results identified specific gait features, which may contribute to pathological femoral growth. Furthermore, the hip joint contact force orientation in the sagittal plane seems to be the dominant factor for determining femoral growth simulations.

1. Introduction

Cerebral palsy (CP) is the most common pediatric neurologic disorder with a prevalence of 2–3 cases per 1000 live births in Europe (Odding et al., 2006). Neuro-musculoskeletal abnormalities in children with CP result in progressive disabilities in performing daily activities, with walking impairments being one of the most profound (Wren et al., 2005). Many children with CP develop skeletal deformities during childhood (Beals, 1969; Bobroff et al., 1999; Morrell et al., 2002). So far, it is unknown why some children with CP develop bony deformities whereas others do not.

At the femur, the anteversion and neck-shaft angle are the two most important anatomical features (Sangeux, 2019). Anteversion angle (AVA) is the angle in the transverse plane by which the neck of the femur deviates forwards from the axis of the femoral condyles. The neck-shaft angle (NSA) is the angle between the neck and the shaft of the femur. In typically developing (TD) children, femoral AVA decreases from approximately 40° at birth to 15° at skeletal maturity, whereas the NSA decreases from 140° to 125°. Although children with CP are born without skeletal pathology, the AVA and NSA often show little change during childhood and therefore can lead to differences up to 50° compared to the values of TD children (Bobroff et al., 1999; Fabry et al., 1973; Robin et al., 2008). Differences in femoral

* Corresponding author at: Centre for Sport Science and University Sports, Department of Biomechanics, Kinesiology, and Computer Science in Sport, University of Vienna, Auf der Schmelz 6a, 1150 Vienna, Austria.
E-mail address: hans.kainz@univie.ac.at (H. Kainz).

https://doi.org/10.1016/j.clinbiomech.2021.105405
Received 22 December 2020; Accepted 1 June 2021
Available online 5 June 2021

development between CP and TD children are hypothesized to be related to delayed onset of walking as well as to altered femoral loading conditions given the aberrant gait kinematics (Fabry et al., 1973; Robin et al., 2008; Shefelbine and Carter, 2004), which influence the remodeling of the femur (Tayton, 2007).

A multi-scale modelling approach, which combines musculoskeletal simulations with mechanobiological finite element analysis, can be used to predict femoral growth trends (Carriero et al., 2011; Kainz et al., 2020; Yadav et al., 2016). Carriero et al. (2011) simulated femoral growth and confirmed increased NSA and AVA in three children with CP when compared to a TD child. Yadav et al. (2016) analyzed the impact of growth plate geometry and different growth direction models on simulation results in one TD child. Their results showed that including a subject-specific growth plate only slightly changed the predicted NSA and AVA compared to using a generic-simplified growth plate, whereas the different growth direction models had a big impact on predicted AVA. Yadav et al. (2017) investigated the impact of muscle groups' activation on simulated proximal femoral growth in three TD children and showed that hip abductors contributed the most, and hip adductors, the least, to growth rate. Kainz et al. (2020) evaluated the impact of initial NSA and AVA on femoral growth simulations and found similar growth rates but different growth directions between models of femoral growth. All these studies increased our insights in the mechanobiology of femoral growth. However, only very small sample sizes ($n = 1$ to 4) were included in the previous studies and, therefore, generalization of the research insights to a heterogenous clinical population, such as CP, was limited. Nevertheless, the mechanobiological workflow holds a unique potential to evaluate the effect of inter-subject variability in gait kinematics and musculoskeletal loading on femoral growth.

The aims of this study were to (i) investigate what loading characteristics underlie typical and pathological femoral growth simulations, and (ii) determine the gait kinematics that differentiate both simulations. To address these aims, a previously developed multi-scale workflow was used to simulate femoral growth in six TD children and 16 children with CP. We hypothesized that (i) hip joint contact forces, which are known to have the largest impact on femoral growth (Yadav et al., 2017), differ between typical and pathological growth simulations, and (ii) specific gait patterns can be identified that differentiate both. These insights are important as they may in future help in discriminating between children with CP who are likely to develop femoral deformities and who not.

2. Methods

A multi-scale modelling workflow was used to simulate femoral growth. First, we modified the NSA and AVA of a generic musculoskeletal model to create a generic child-specific model with a NSA of 140° and an AVA of 30°, which was used to calculate subject-specific joint kinematics and femoral loading based on the motion capture data from each participants. Second, a finite element model of the femur from our previous study (Kainz et al., 2020) was modified to match the NSA and AVA of the generic child-specific musculoskeletal model and used for mechanobiological simulations based on the subject-specific loading of each child. Third, we divided our participants with CP into a typical and pathological growth group based on the predicted growth trends from our simulations. Forth, joint kinematics and femoral loading were compared between our TD and both CP groups to answer our research questions.

2.1. Participants

Three-dimensional motion capture data of six TD children and 16 children diagnosed with spastic diplegic CP were retrospectively analyzed in this study. We have analyzed and reported dynamic muscle forces in these participants (Kainz et al., 2019; Wesseling et al., 2020) but we have not previously published investigations on femoral growth. Participants with CP were able to walk without an assistive device for at least 10 m and had a Gross Motor Function Classification System (GMFCS) score of I or II. Detailed characteristics of all participants are shown in Table 1. Ethical clearance to use the retrospective data was obtained from the local Ethical Committee (UZ Leuven, Belgium, S57746).

2.2. Motion capture data

The motion capture data of our participants included marker trajectories of the Plug-in-Gait lower limb marker set (Kadaba et al., 1990) and force plate data of one static trial and several walking trials at a self-selected walking speed. A 10–15 camera motion capture system (Vicon Motion Systems, Oxford, UK) and two force plates (AMTI, Watertown, MA, USA) were used to record the data.

2.3. Musculoskeletal simulations

Joint kinematics, joint kinetics, muscle and joint contact forces (JCF) were calculated in OpenSim 3.3 (Delp et al., 2007) using a model with child-specific femoral geometry. The deform tool in SIMM (Arnold et al., 2001) was used to change the NSA and AVA of a generic musculoskeletal SIMM model (Delp et al., 1990) to child-specific values of 140° and 30°, respectively. The torso segment and corresponding muscles were removed from the model and the subtalar and metatarsophalangeal joints locked due to insufficient markers to track these joints. The final model included 16 degrees-of-freedom (six at the pelvis, three at each hip and one at each knee and ankle joint) and 88 muscles and was scaled to the body mass and segment lengths of each participant based on the marker locations from the static trial and estimated joint centers (Kainz et al., 2017). Inverse Kinematics and Inverse Dynamics were used to calculate joint kinematics and joint kinetics, respectively. Muscle forces were calculated using static optimization, while minimizing the sum of squared muscle activations. Finally, OpenSim's joint reaction analysis (Steele et al., 2012) was used to estimate JCF. Hip JCF were reported in the segment reference frame of the femur, whereas knee JCF were reported in the segment reference frame of the tibia (Supplementary Fig. S1).

2.4. Finite element model

A previously developed finite element (FE) femur model (Kainz et al., 2020) based on magnetic resonance images (MRI) of an 8-year-old child was modified to match the NSA and AVA of the average child-specific musculoskeletal model. This FE model was used for the mechanobiological simulations of all participants. A detailed description of the workflow to create the FE model is provided in our previous publication (Kainz et al., 2020). The final FE model included a pure hexahedral mesh with seven rows of elements representing the growth plate. In agreement with previous studies (Carriero et al., 2011; Kainz et al., 2020; Yadav et al., 2017), material properties were chosen to be elastic, isotropic and homogenous with a modulus of elasticity of 20,000 MPa, 1 MPa, 600 MPa, 2942 MPa and 6 MPa for the cortical bone, bone marrow, proximal trabecular bone, distal trabecular bone and growth plate, respectively. Ten rows above and below the proximal growth plate formed a transition zone with a linearly decreasing elastic modulus from 600 and 6 MPa. Poisson's ration of 0.3 was chosen for all anatomical structure except the growth plate, which had a Poisson's ration of 0.48.

2.5. Mechanobiological simulations

Mechanobiological growth simulations were performed based on a previously developed workflow (Carriero et al., 2011) and is described in detail in our previous paper (Kainz et al., 2020). The FE model was created based on MRI images of a child with a body weight of 20.4 kg. Hence, muscle and JCF from the musculoskeletal simulations were first normalized to the body weight of each participant and afterwards multiplied with the body weight of the child from whom the FE model was built. This allowed comparisons of force magnitudes across all

Table 1
Participant characteristics across the three analyzed groups (TD, CP-TDgrowth and CP-PathGrowth).

TD	age (years)	weight (kg)	height (mm)	Gender (F/M)	Gait velocity	LLI (cm)
1	9	32	1340	M	0.65	−1.1
2	9	28	1340	M	0.44	0.7
3	7	23	1270	M	0.56	0.2
4	7	19	1160	M	0.34	−0.6
5	10	38	1407	F	0.48	−0.7
6	10	29	1314	F	0.47	−0.4
mean	9	28	1305	2 F / 4 M	0.49	−0.3
SD	1	6	77		0.10	0.6

CP-TDgrowth	age (years)	weight (kg)	height (mm)	Gender (F/M)	Gait velocity	LLI (cm)	GMFCS level
1	7	21	1147	F	0.47	−1.0	II
2	6	28	1230	F	0.36	−0.1	II
3	7	23	1281	F	0.43	0.5	I
4	8	22	1229	M	0.41	0.1	II
5	8	22	1252	F	0.42	−0.9	I
6	9	26	1300	F	0.44	−0.2	I
7	10	25	1267	M	0.45	1.1	II
8	14	37	1591	F	0.40	−0.7	II
mean	8	25	1287	6 F / 2 M	0.42	−0.1	I: 3, II: 5
SD	2	5	123		0.03	0.7	

CP-PathGrowth	age (years)	weight (kg)	height (mm)	Gender (F/M)	Gait velocity	LLI (cm)	GMFCS level
1	11	32	1382	F	0.40	1.2	II
2	7	29	1216	M	0.34	0.3	II
3	8	29	1240	M	0.43	0.4	II
4	7	35	1261	M	0.34	0.0	II
5	12	41	1532	M	0.45	0.9	II
6	6	19	1171	M	0.62	1.1	II
7	9	29	1317	F	0.28	−0.4	II
8	10	32	1346	M	0.38	0.9	II
mean	9	31	1308	6 M / 2 F	0.41	0.6	II: 8
SD	2	6	107		0.10	0.5	

F = female; M = male; SD = standard deviation. LLI = leg length inequality (left minus right leg). Leg length was quantified based on the distance between the hip and ankle joint centres obtained from marker positions of the static trial of each participant. All children with CP were diagnosed with spastic diplegic CP.

participants. Hip JCF and muscle forces acting on the femur from nine sequential instances during the stance phase were used to define the loading scenario in the FE model. The position of the femoral condyles was fixed in all directions. Within a first FE analysis, growth rate was defined as the osteogenic index and calculated for each element of the distal layer of the growth plate based on the minimum hydrostatic stress and maximum octahedral shear stress at the proximal growth plate. To reduce computational time and still see clear differences in growth trends, the obtained growth rates were multiplied with a constant scale factor. Growth direction was defined as the average deformation of the femoral neck. In a second FE analysis, femoral growth was simulated using orthonormal thermal expansion based on a temperature load defined by the calculated growth rate for each element and in the direction of the average deformation of the neck. Afterwards, the nodal coordinates of the whole femur were updated and the final geometry (NSA and AVA) was compared to the original geometry of the FE model. FE analyses were performed in Abaqus (2017, Simulia, UK) in combination with customized Python and Matlab scripts.

2.6. Data analysis

We first simulated femoral growth and calculated the change in NSA and AVA for all our participants. Based on the simulated growth results, we divided our participants with CP into two groups: (1) CP-TDgrowth group: simulated change in NSA and AVA were within or above the mean ± two standard deviations values of our TD simulations, indicating both NSA and AVA decreased as much or more than TD; and (2) CP-PathGrowth group: change in NSA and/or AVA were below the mean ± two standard deviations values of our TD participants, indicating NSA and AVA did not change as much as TD.

We examined the hip JCF vector in order to understand how gait kinematics affect JCF. Previous simulations have shown that the hip JCF ($\vec{R}_{hip}$, Eq. 1 (Steele et al., 2012) has a larger impact on femoral growth compared to muscle forces (Yadav et al., 2017).

$$\vec{R}_{hip} = [M]_{femur}\,\vec{a}_{femur} - \left(\vec{R}_{knee} + \vec{F}_{gravity} + \sum \vec{F}_{muscles\_femur}\right) \quad (1)$$

Considering the relative small mass ($[M]_{femur}$) and accelerations ($\vec{a}_{femur}$) of the femur during walking, mainly the knee JCF ($\vec{R}_{knee}$) and muscle forces attached to the femur ($\sum \vec{F}_{muscles\_femur}$) influence hip JCF. We compared hip JCF orientation and magnitude, knee JCF, and muscle forces acting on the femur between TD children and CP-PathGrowth group (research question 1) and between the CP-TDgrowth and CP-PathGrowth groups (research question 2). Additionally, we compared joint kinematics and walking velocities between different groups to investigate what kinematic features may cause the differences in femoral loading and growth simulations. Walking velocity was normalized to leg length as proposed by Hof (1996) using Eq. 2.

$$v^{*} = \frac{v}{\sqrt{gL_{leg}}} \quad (2)$$

v^{*} in Eq. 2 is the dimensionless walking speed normalized to leg length (L_{leg}). v is the walking velocity in m/s and g is gravity (9.81 m/s^2). Statistical Parametric Mapping (SPM) (Pataky, 2010) based on the SPM1D package for Matlab (http://www.spm1d.org/) was used to compare hip JCF, knee JCF, muscle forces acting on the femur and joint kinematics between the different groups. The Hotelling's T^2 test, SPM's vector field analog to the two-sampled t-test, with an alpha level of 0.05 was used to analyze the entire vector field (e.g. all three planes of the hip

kinematics). In case of a significant difference, post hoc two-tailed scalar trajectory *t*-tests (SPM{t}) with Bonferroni adjusted alpha level in case of multiple comparisons (e.g. $p = 0.05/3 = 0.0167$ for hip joint angles in each plane) were conducted on each vector component separately (Pataky et al., 2013). SPM analyses were performed over the entire kinematic waveforms, whereas only the stance phase (0% to 60% of the gait cycle) was included for the comparison of JCF and muscle forces. Hip JCF orientation was calculated as the average orientation during the stance phase of the gait cycle. Hip JCF orientations and walking velocities were compared between the different groups using independent t-tests.

3. Results

Growth simulation led to an average (standard deviation) decrease in AVA of 0.34° (0.09°) and 0.32° (0.12°) in TD and CP simulations, respectively. The average decrease in NSA was 0.77° (0.01°) in our TD simulations compared to 0.74° (0.02°) the CP simulations. Dividing the CP group based on the growth simulation resulted in an even distributed number ($n = 8$) between both groups. The average decrease in AVA and NSA was 0.40° (0.05°) and 0.76° (0.02°) in the CP-TDgrowth, respectively, and 0.23° (0.10°) and 0.73° (0.02°) in the CP-PathGrowth group (Fig. 1).

3.1. TD versus CP-PathGrowth

Mean hip JCF orientation in the sagittal and frontal plane was significantly ($P < 0.05$) different in our TD versus CP-PathGrowth simulations. The mean hip JCF orientation in the frontal plane of the CP-PathGrowth was, however, within the average ± two standard deviation range of our TD participants (Fig. 2).

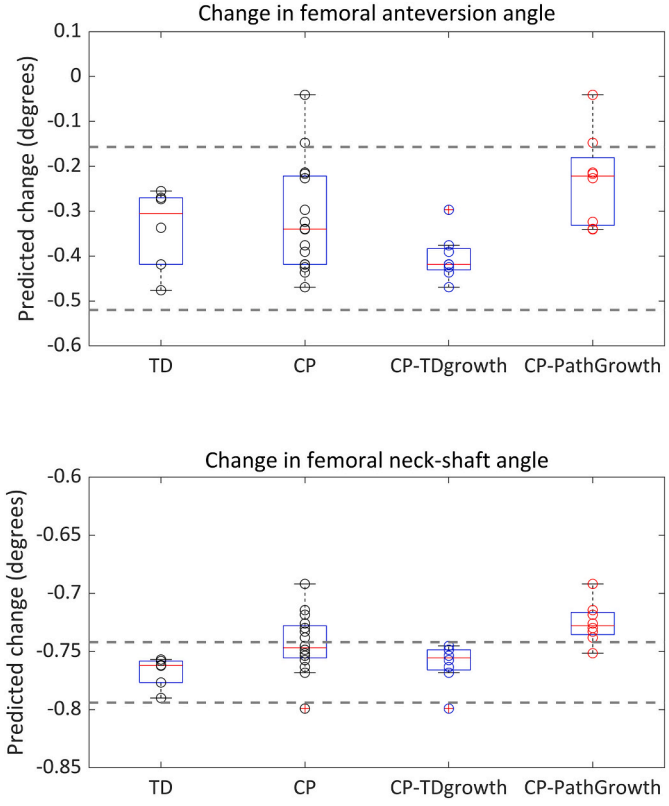

Fig. 1. Predicted change in femoral anteversion and neck-shaft angle for all analyzed participant groups. Dashed horizontal lines indicate the average ± two standard deviation values of our typically developing participants. The CP group ($n = 16$) was divided into the CP-TDgrowth (n = 8) and CP-PathGrowth (n = 8) groups.

During the stance phase of the gait cycle, hip JCF in the posterior and inferior direction were significantly lower ($P < 0.01$) at terminal stance in the CP-PathGrowth group compared to TD, whereas knee JCF in anterior direction were significant higher ($P = 0.005$) during loading response in our CP- PathGrowth group (Fig. 3). Muscle forces acting on the femur were significantly ($p < 0.001$) lower in medial direction during terminal stance in the CP-PathGrowth group.

Joint kinematics were significantly different between both groups for knee flexion, hip flexion and ankle plantarflexion angles (Fig. 4). The CP-PathGrowth group presented less hip extension during terminal swing ($P < 0.017$), a significantly increased knee flexion during loading response ($P = 0.005$) and terminal swing ($P < 0.001$), as well as significantly increased ankle dorsiflexion during loading response ($P = 0.01$). Dimensionless walking velocity was higher in the TD simulations (0.49 ± 0.10) compared to the CP- PathGrowth group (0.41 ± 0.10) but the difference was not significant.

3.2. CP-TDgrowth versus CP-PathGrowth

Mean hip JCF orientation in the sagittal plane was significantly less posterior oriented ($P = 0.003$) in the CP-PathGrowth compared to the CP-TDgrowth group. Sagittal plane hip JCF orientations of the CP-TDgrowth group were similar to the TD values (Fig. 2).

Posterior ($P < 0.001$), inferior ($P < 0.01$) and lateral ($P < 0.011$) hip JCF around midstance were significantly higher in the CP-TDgrowth compared to the CP-PathGrowth group. Knee JCF in inferior direction ($P = 0.002$) and muscle forces acting on the femur in medial direction ($P < 0.001$) were also significantly higher around midstance in the CP-TDgrowth group (Fig. 3, supplementary Fig. S5).

Pelvic ($P < 0.001$) and hip kinematics ($P = 0.001$) in the frontal plane were significantly different between the CP-TDgrowth and CP-PathGrowth groups: The CP-TDgrowth group presented an increased pelvic obliquity (pelvis was more up) compared to the CP-PathGrowth group. Furthermore, the hip was more adducted during midstance in the CP-TDgrowth group (Fig. 4). Dimensionless walking velocity was not significant different between the CP-TDgrowth (0.42 ± 0.03) and CP-PathGrowth (0.41 ± 0.10) groups.

4. Discussion

The aim of this study was to address two clinically relevant research questions using a multi-scale simulation workflow. To identify the loading characteristic leading to TD and pathological femoral growth, we compared hip joint loading between the TD and CP-PathGrowth groups. In agreement with our first hypothesis, we found different hip JCF characteristics between simulations with TD and pathological femoral growth. Hip JCF were lower in magnitude and less posterior oriented in the CP-PathGrowth group. In regards to our second research question that focusses on reasons for typical versus pathological growth in CP simulations, we found that the pelvic and hip movement strategy in the frontal plane differed between the CP-TDgrowth and CP-PathGrowth groups, which led to different femoral loading pattern and, therefore, different hip JCF orientation. These findings confirmed our second hypothesis.

Our joint kinematics and JCF results are in agreement with previous studies. Simulation results of our TD participants showed typical joint kinematic waveforms (Schwartz et al., 2008) and hip and knee JCF (Modenese et al., 2018). The increased knee and hip flexion observed in the joint kinematics of our participants with CP are common gait abnormalities in children with CP (Wren et al., 2005). Furthermore, the increased knee JCF and decreased hip JCF in our participants with CP are in agreement with previous simulation studies (Steele et al., 2012; Van Rossom et al., 2020).

Different gait pattern changed the loading environment and, therefore, the growth results in our simulation groups (Fig. 5). Which gait features were responsible for specific alterations in the loading environment is difficult to assess due to the redundant musculoskeletal system and the

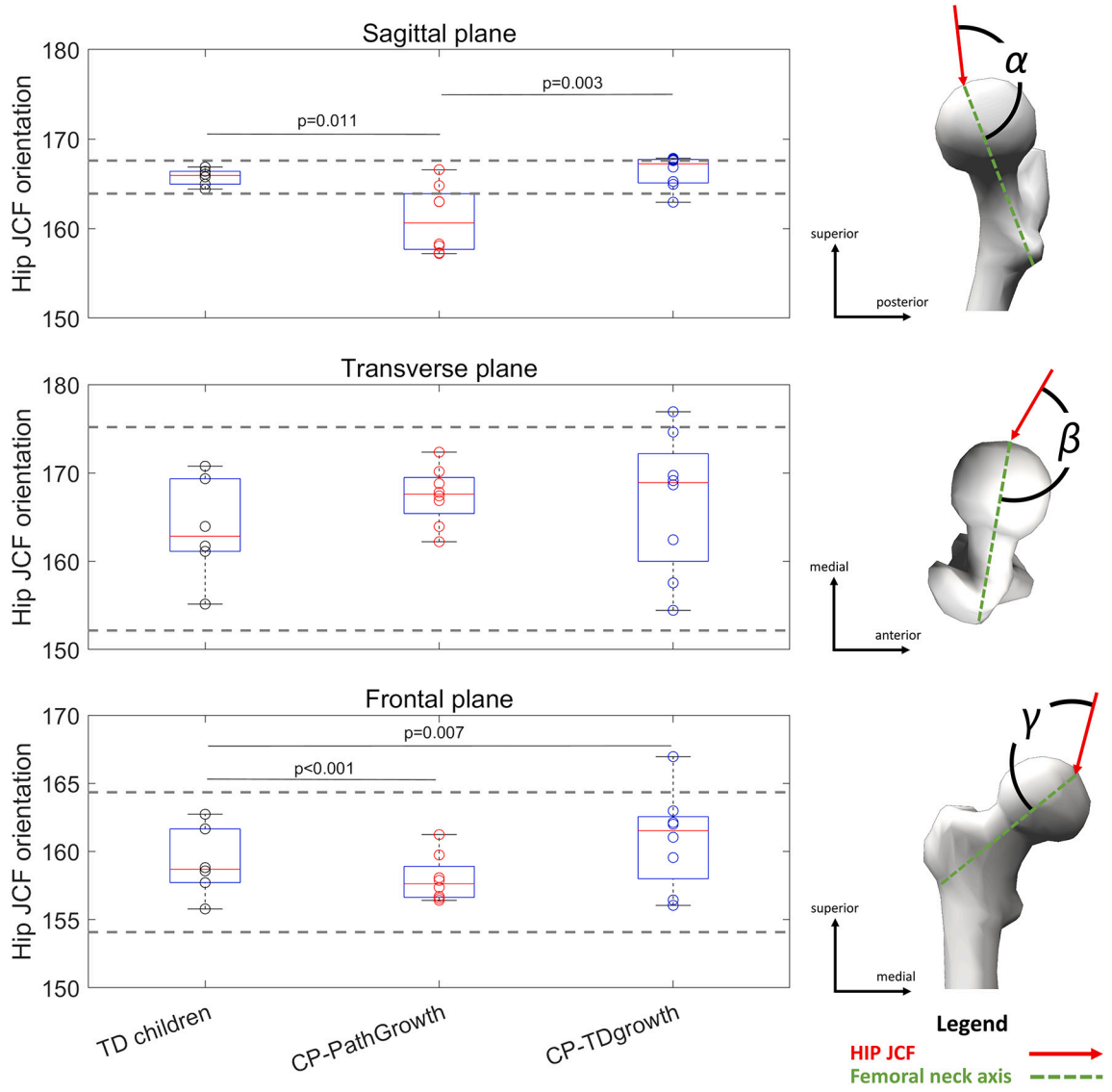

Fig. 2. Hip joint contact force (JCF) orientation for our TD children and both CP groups. Dashed horizontal lines indicate the average ± two standard deviation values of our typically developing participants. α, β and γ indicate the angles to define the hip JCF orientation in the sagittal, transverse and frontal plane, respectively.

numerous parameters involved in the calculation of hip JCF. For example, compared to our TD participants, the CP-PathGrowth group walked with increased knee flexion and decreased hip extension during the whole stance phase. Reduced hip extension leads to a decreased hip flexion moment (supplementary Fig. S2), which potentially explains the decreased anterior-pulling muscle forces in the CP-PathGrowth group. Furthermore, the decrease in anterior-pulling muscle forces at the femur could cause the decrease in posterior hip JCF (Eq. 1) and, therefore, changed the mean hip JCF orientation in the sagittal plane and lead to pathological femoral growth results as shown in our findings. This potential interpretation, however, is not supported by a mechanistic analysis. Musculoskeletal forward simulations (Falisse et al., 2020) could provide insights in the gait compensations introduced by specific coordination deficits and muscle weakness and their consequent effect on hip loading and femoral growth.

Despite pathological sagittal plane kinematics in both CP groups, differences in frontal plane pelvic and hip kinematics led to typical femoral growth in the CP-TDgrowth group. This suggest that the loading environment can be normalized even in the presence of pathological sagittal plane kinematics. Furthermore, only a subset of the loading parameters normalized in the CP-TDgrowth compared to CP-PathGrowth group (Fig. 5) and therefore differentiated between typically developing and pathological femoral growth. In the CP-TDgrowth group, hip JCF as well as medially-directed muscle forces were higher and sagittal plane hip JCF was more posterior-oriented compared to the CP-PathGrowth group. Hence, it seems that these parameters are the key players in determining growth trends under the given modelling assumptions.

Previous research showed that an increasing walking velocity alters gait kinematics (Schwartz et al., 2008) and increases hip JCF (Giarmatzis et al., 2015). The decreased hip JCF in the CP-PathGrowth compared to the TD and CP-TDgrowth groups could, therefore, be caused by differences in the walking velocity. Dimensionless walking velocity was, indeed, higher in the TD participants compared to the CP-PathGrowth group. The walking velocity was, however, not different between both CP groups although hip JCF were significantly higher in the CP-TDgrowth compared to the CP-PathGrowth group. Hence, the different pelvic and hip kinematics together with the associated different muscle activity were likely the reasons for the differences in hip JCF.

In the current study mechanobiological simulation based on motion capture data of 22 children (6 TD children +16 children with CP) were

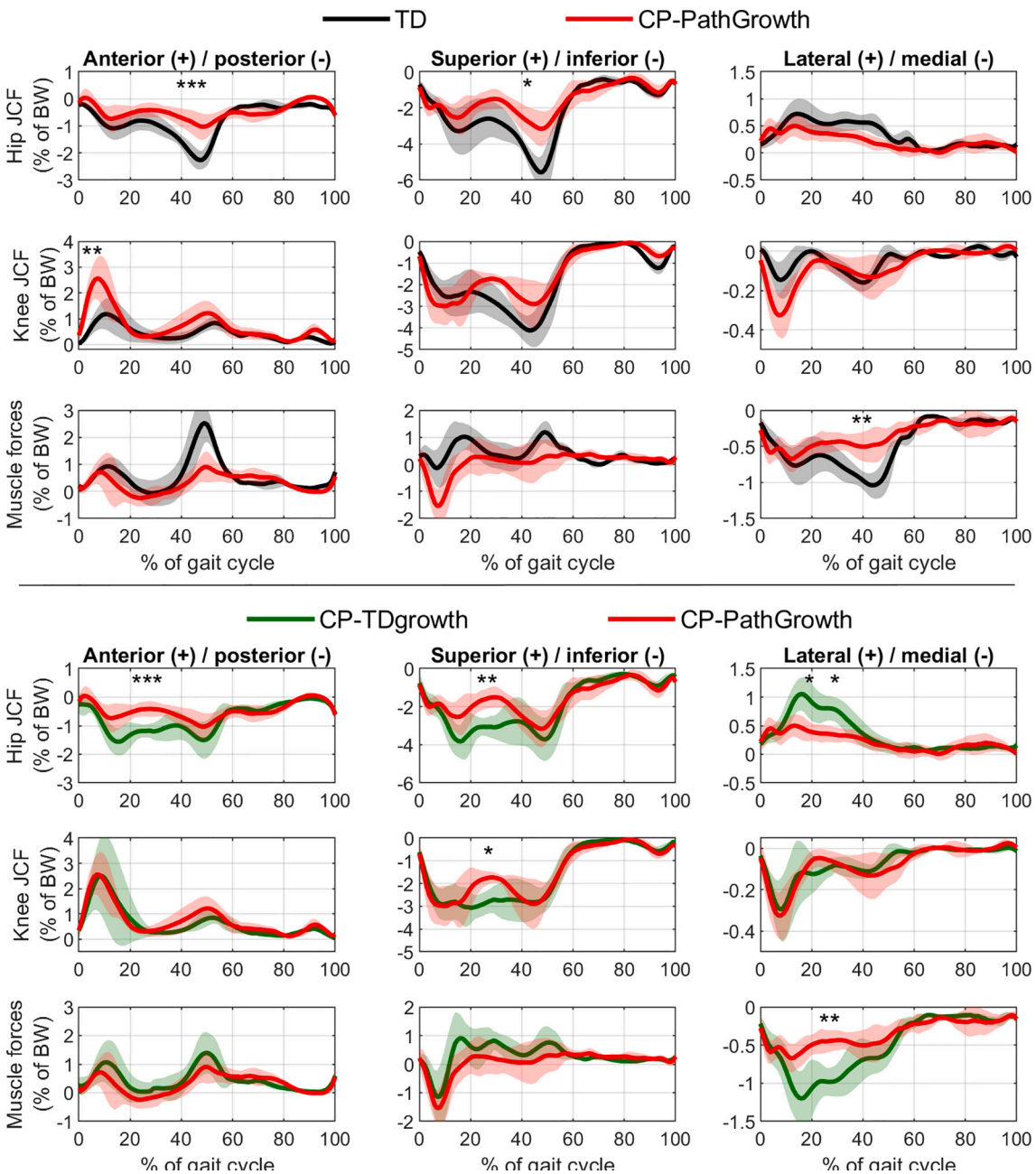

Fig. 3. Hip joint contact force (JCF), knee JCF and muscle forces acting on the femur for the comparison of the TD participants with the CP-PathGrowth group (top three rows) and the comarison between the CP-TDgrowth and CP-PathGrowth groups (bottom three rows). * indicate significant differences based on the SPM analysis. The hip JCF and muscle forces were reported in the segment reference frame of the femur, whereas knee JCF were reported in the segment reference frame of the tibia (supplementary Fig. S1).

used to answer our research questions. Our sample size is more than five-times the sample size of any previous conducted studies related to femoral growth simulations in children. Nevertheless, the majority of our participants with CP walked with an apparent equinus gait pattern according to the Rodda-Graham classification (Fig. 4), which is only representative for a subset of children with CP (Rodda and Graham, 2001). The evaluation of inter-subject variability of simulation results is an important step to get confidence in the multi-scale modelling workflow (Viceconti et al., 2005). In general, we found lower inter-subject variability for predicted changes in NSA than for predicted AVA. Before the workflow can be used in a clinical setting, we need to validate the accuracy of the prediction. This, however, was beyond the scope of the current study as it would require longitudinal medical images and motion capture data.

The mean hip JCF orientation in the sagittal plane seems to play an important role in determining femoral growth trends. Inter-subject variability of the hip JCF orientation in the sagittal plane was very small (standard deviation of 0.9°) in our TD simulations (Fig. 2), whereas the inter-subject-variability over all CP simulations was more than four-times of the TD value (standard deviation of 4.0°). Considering the high variability in CP gait patterns, this was not a surprising finding.

Alterations in the hip JCF orientation is associated with femoral growth trends. This information could be used to inform clinical interventions in the future. For example, movement therapies assisted by real-time biofeedback based on musculoskeletal simulation (similar to Pizzolato et al., 2020) could be used to alter key biomechanical parameters (i.e. hip JCF orientation) to normalize growth trends. Such an approach has a huge potential and could revolutionize clinical decision-

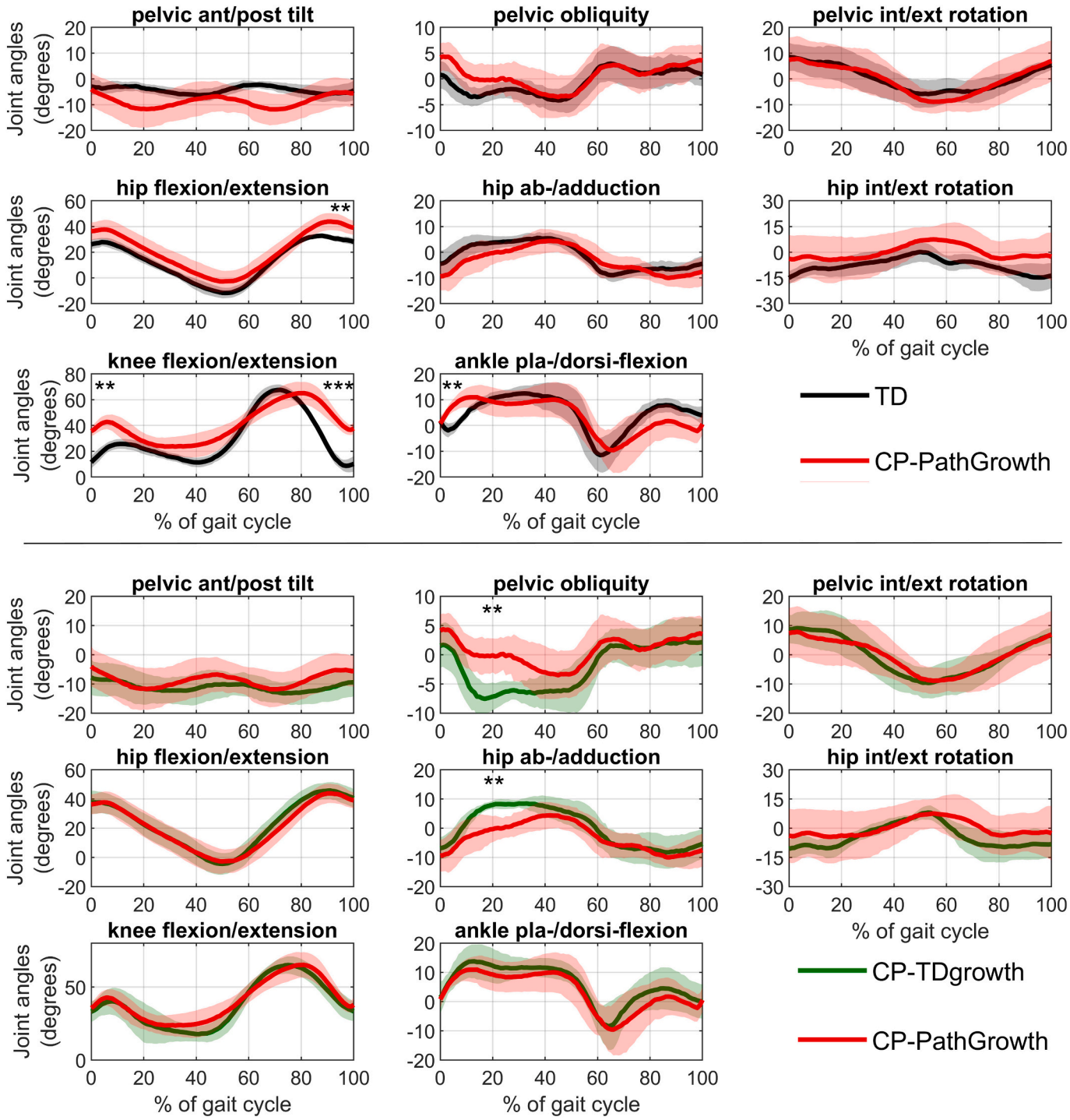

Fig. 4. Joint kinematics for the comparison of the TD participants with the CP-PathGrowth group (top three rows) and the comarison between the CP-TDgrowth and CP-PathGrowth groups (bottom three rows). * indicate significant differences based on the SPM analysis.

making in the future. Further validation of the used workflow is, however, needed before precise clinical recommendation can be made.

In our CP-PathGrowth group we found a less pronounced pelvic obliquity combined with a hip abduction during the first part of the gait cycle compared to both other groups. This is a common observed gait feature in some children with CP and is believed to be related to hip muscle weakness (Krautwurst et al., 2013; Metaxiotis et al., 2000). Based on our simulation results, it seems that this gait pattern also contributes to altered hip JCF orientations and, therefore, pathological femoral growth. As some children with CP develop asymmetric deformities with hip adduction on one side and hip abduction on the other side, i.e. windswept hip deformities (Morrell et al., 2002), it would be interesting to know how joint loading and consequently femoral growth simulation would differ between both sides in patients with asymmetric deformities. Considering that windswept hip deformities are mostly seen in non-ambulatory children, advanced measurement techniques would be necessary to estimate reaction forces for the multi-scale modelling workflow.

Leg length inequalities could be the reason for the less pronounced pelvic obliquity in our CP-PathGrowth group. Maximum leg length discrepancies of all our participants were below 12 mm, which is clearly

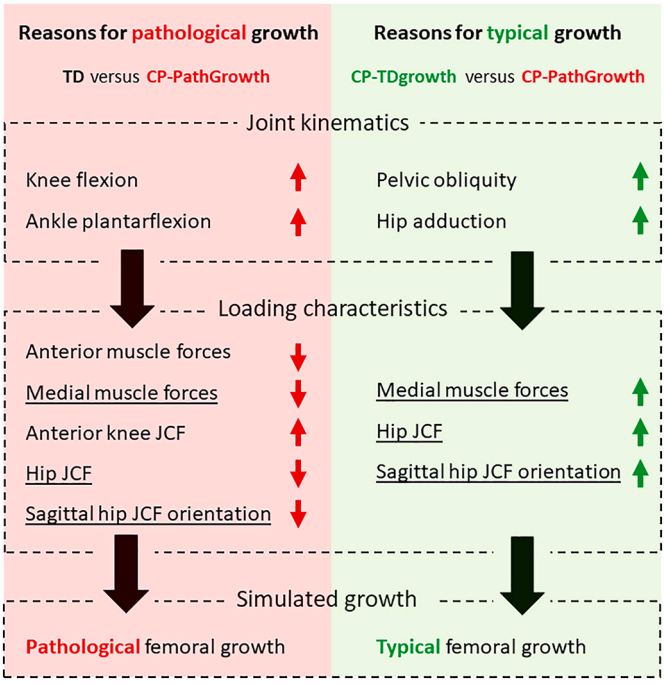

Fig. 5. Summary of potential reasons for pathological and typical femoral growth based on the findings of our multi-scale simulations. Underlined parameters highlight parameters which seemed to play an important role in both comparisons. TD = typically developing; JCF = joint contact force; red/green arrow up = increase; red/green arrow down = decrease. (For interpretation of the references to colour in this figure legend, the reader is referred to the web version of this article.)

below the clinically significant threshold of 20 mm (Knutson, 2005) and, therefore, unlikely affected our growth predictions. Nevertheless, the left was longer than the right leg in all except of one participant in the CP-PathGrowth group (Table 1). Future studies should evaluate the cause-effect relationship between leg length inequalities and the development of femoral deformities.

In TD children, the average decrease in femoral AVA and NSA between the age of eight and ten years is around 2° and 1°, respectively (Bobroff et al., 1999; Robin et al., 2008). Our simulations would, therefore, roughly account for growth over a duration of eleven months. Femoral NSA decreased more than the AVA in our participants, which is in contrast to previous cross-sectional studies based on measured femoral geometry (Bobroff et al., 1999; Robin et al., 2008). Evaluating the reason for the discrepancies was beyond the scope of this study. Future studies based on medical images collected from children on two occasions are needed to validate some of the modelling assumptions and quantify the accuracy of the growth simulations.

Our simulation approach included some limitations. First, we used a child-specific musculoskeletal and finite element model but did not include subject-specific geometry details of each participant (e.g. growth plate alignment and thickness, NSA and AVA) due to the lack of medical images. Subject-specific growth plate (Yadav et al., 2016) and femoral geometry (Kainz et al., 2020) has been shown to influence simulation results and, therefore, growth results will likely differ if subject-specific models are used for the simulations. Using an identical model for each participant, it, however, was possible to isolate the key kinematic and kinetic parameters related to femoral growth, independent of femoral initial geometry. Even if the absolute values of our simulation results are not accurate, the difference in growth results, femoral loading and gait pattern let us draw some clinically relevant conclusions on a group level. Second, similar to previous femoral growth studies (Carriero et al., 2011; Kainz et al., 2020; Yadav et al., 2016), the greatly simplified material properties and chosen loading scenario do not represent the real human femur and loading pattern during all activities of daily living. Children usually perform a vast variety of movements, which could influence the stresses on the growth plate and therefore femoral growth. These simplifications are, however, acceptable for studying the mechanobiology of the growth plate (Carter and Wong, 2003). Third, we chose to simulate growth in the direction of the average deformation of the femoral neck based on our previous study (Kainz et al., 2020). Different algorithm to define the growth direction (Yadav et al., 2016) or growth amount might change the absolute values of our simulations. Forth, we only simulate growth at the proximal growth plate and neglected growth at the distal and trochanter growth plates. Furthermore, choosing different threshold to define pathological and TD growth might slightly change our findings. Fifth, our musculoskeletal simulations were based on linear-scaled generic models, which include scaling uncertainties (Koller et al., 2021), limited degrees-of-freedom at the knee and ankle joint due to the available marker set (Kainz et al., 2016), and a simplified muscle architecture due to discretization of the muscle lines of action (Modenese and Kohout, 2020). Furthermore, we used static optimization to estimate muscle forces and, therefore, neglected the subject-specific motor control of our participants (Veerkamp et al., 2019). Future studies should investigate how these modelling details influence femoral growth simulations.

5. Conclusions

Our multi-scale simulation results showed that a less posterior-oriented hip JCF is likely the dominant factor for pathological femoral growth. Within the simulations of CP gait, altered pelvic and hip movement strategy in the frontal plane led to a normalization of the hip JCF and, therefore, typical femoral growth even in the presence of pathological sagittal plane kinematics. Our workflow (models and scripts) is made freely available on https://simtk.org/projects/normal-load.

Acknowledgements

This project was partly funded by an IWT-TBM grant (140184) and a H2020-MSCA individual fellowship (796120).

Appendix A. Supplementary data

Supplementary data to this article can be found online at https://doi.org/10.1016/j.clinbiomech.2021.105405.

References

Arnold, A.S., Blemker, S.S., Delp, S.L., 2001. Evaluation of a deformable musculoskeletal model for estimating muscle–tendon lengths during crouch gait. Ann. Biomed. Eng. 29, 263–274. https://doi.org/10.1114/1.1355277.

Beals, R.K., 1969. Developmental changes in the femur and acetabulum in spastic paraplegia and Diplegia. Dev. Med. Child Neurol. 11, 303–313. https://doi.org/10.1111/j.1469-8749.1969.tb01437.x.

Bobroff, E.D., Chambers, H.G., Sartoris, D.J., Wyatt, M.P., Sutherland, D.H., 1999. Femoral anteversion and neck-shaft angle in children with cerebral palsy. Clin. Orthop. Relat. Res. 194–204.

Carriero, A., Jonkers, I., Shefelbine, S.J., 2011. Mechanobiological prediction of proximal femoral deformities in children with cerebral palsy. Comput. Methods Biomech. Biomed. Engin. 14, 253–262. https://doi.org/10.1080/10255841003682505.

Carter, D.R., Wong, M., 2003. Modelling cartilage mechanobiology. Philos. Trans. R. Soc. Lond. Ser. B Biol. Sci. 358, 1461–1471. https://doi.org/10.1098/rstb.2003.1346.

Delp, S.L., Loan, J.P., Hoy, M.G., Zajac, F.E., Topp, E.L., Rosen, J.M., 1990. An interactive graphics-based model of the lower extremity to study orthopaedic surgical procedures. IEEE Trans. Biomed. Eng. 37, 757–767. https://doi.org/10.1109/10.102791.

Delp, S.L., Anderson, F.C., Arnold, A.S., Loan, P., Habib, A., John, C.T., Guendelman, E., Thelen, D.G., 2007. OpenSim: open-source software to create and analyze dynamic simulations of movement. IEEE Trans. Biomed. Eng. 54, 1940–1950. https://doi.org/10.1109/TBME.2007.901024.

Fabry, G., MacEwen, G.D., Shands, A.R., 1973. Torsion of the femur A follow up study in normal and abnormal conditions. J. Bone Jt. Surg. - Ser. A 55, 1726–1738. https://doi.org/10.2106/00004623-197355080-00017.

Falisse, A., Pitto, L., Kainz, H., Hoang, H., Wesseling, M., Van Rossom, S., Papageorgiou, E., Bar-On, L., Hallemans, A., Desloovere, K., Molenaers, G., Van Campenhout, A., De Groote, F., Jonkers, I., 2020. Physics-based simulations to predict the differential effects of motor control and musculoskeletal deficits on gait

dysfunction in cerebral palsy: a retrospective case study. Front. Hum. Neurosci. 14, 40. https://doi.org/10.3389/fnhum.2020.00040.
Giarmatzis, G., Jonkers, I., Wesseling, M., Van Rossom, S., Verschueren, S., 2015. Loading of hip measured by hip contact forces at different speeds of walking and running. J. Bone Miner. Res. 30, 1431–1440. https://doi.org/10.1002/jbmr.2483.
Hof, A.L., 1996. Scaling gait data to body size. Gait Posture. https://doi.org/10.1016/0966-6362(95)01057-2.
Kadaba, M.P., Ramakrishnan, H.K., Wootten, M.E., 1990. Measurement of lower extremity kinematics during level walking. J. Orthop. Res. 8, 383–392. https://doi.org/10.1002/jor.1100080310.
Kainz, H., Modenese, L., Lloyd, D.G., Maine, S., Walsh, H.P.J., Carty, C.P., 2016. Joint kinematic calculation based on clinical direct kinematic versus inverse kinematic gait models. J. Biomech. 49, 1658–1669. https://doi.org/10.1016/j.jbiomech.2016.03.052.
Kainz, H., Hoang, H.X., Stockton, C., Boyd, R.R., Lloyd, D.G., Carty, C.P., 2017. Accuracy and reliability of marker-based approaches to scale the pelvis, thigh, and shank segments in musculoskeletal models. J. Appl. Biomech. 33, 354–360. https://doi.org/10.1123/jab.2016-0282.
Kainz, H., Hoang, H., Pitto, L., Wesseling, M., Van Rossom, S., Van Campenhout, A., Molenaers, G., De Groote, F., Desloovere, K., Jonkers, I., 2019. Selective dorsal rhizotomy improves muscle forces during walking in children with spastic cerebral palsy. Clin. Biomech. (Bristol, Avon) 65, 26–33. https://doi.org/10.1016/j.clinbiomech.2019.03.014.
Kainz, H., Killen, B.A., Wesseling, M., Perez-Boerema, F., Pitto, L., Garcia Aznar, J.M., Shefelbine, S., Jonkers, I., 2020. A multi-scale modelling framework combining musculoskeletal rigid-body simulations with adaptive finite element analyses, to evaluate the impact of femoral geometry on hip joint contact forces and femoral bone growth. PLoS One 15, e0235966. https://doi.org/10.1371/journal.pone.0235966.
Knutson, G.A., 2005. Anatomic and functional leg-length inequality: A review and recommendation for clinical decision-making. Part I, anatomic leg-length inequality: Prevalence, magnitude, effects and clinical significance. Chiropr. Osteopat. https://doi.org/10.1186/1746-1340-13-11.
Koller, W., Baca, A., Kainz, H., 2021. Impact of scaling errors of the thigh and shank segments on musculoskeletal simulation results. Gait Posture 87, 65–74. https://doi.org/10.1016/j.gaitpost.2021.02.016.
Krautwurst, B.K., Wolf, S.I., Heitzmann, D.W.W., Gantz, S., Braatz, F., Dreher, T., 2013. The influence of hip abductor weakness on frontal plane motion of the trunk and pelvis in patients with cerebral palsy. Res. Dev. Disabil. 34, 1198–1203. https://doi.org/10.1016/j.ridd.2012.12.018.
Metaxiotis, D., Accles, W., Siebel, A., Doederlein, L., 2000. Hip deformities in walking patients with cerebral palsy. Gait Posture 11, 86–91. https://doi.org/10.1016/S0966-6362(00)00043-6.
Modenese, L., Kohout, J., 2020. Automated generation of three-dimensional complex muscle geometries for use in personalised musculoskeletal models. Ann. Biomed. Eng. 48, 1793–1804. https://doi.org/10.1007/s10439-020-02490-4.
Modenese, L., Montefiori, E., Wang, A., Wesarg, S., Viceconti, M., Mazzà, C., 2018. Investigation of the dependence of joint contact forces on musculotendon parameters using a codified workflow for image-based modelling. J. Biomech. 73, 108–118. https://doi.org/10.1016/j.jbiomech.2018.03.039.
Morrell, D.S., Pearson, J.M., Sauser, D.D., 2002. Progressive bone and joint abnormalities of the spine and lower extremities in cerebral palsy. RadioGraphics 22, 257–268. https://doi.org/10.1148/radiographics.22.2.g02mr19257.
Odding, E., Roebroeck, M.E., Stam, H.J., 2006. The epidemiology of cerebral palsy: incidence, impairments and risk factors. Disabil. Rehabil. 28, 183–191. https://doi.org/10.1080/09638280500158422.
Pataky, T.C., 2010. Generalized n-dimensional biomechanical field analysis using statistical parametric mapping. J. Biomech. 43, 1976–1982. https://doi.org/10.1016/j.jbiomech.2010.03.008.
Pataky, T.C., Robinson, M.A., Vanrenterghem, J., 2013. Vector field statistical analysis of kinematic and force trajectories. J. Biomech. 46, 2394–2401. https://doi.org/10.1016/j.jbiomech.2013.07.031.
Pizzolato, C., Shim, V.B., Lloyd, D.G., Devaprakash, D., Obst, S.J., Newsham-West, R., Graham, D.F., Besier, T.F., Zheng, M.H., Barrett, R.S., 2020. Targeted achilles tendon training and rehabilitation using personalized and real-time multiscale models of the neuromusculoskeletal system. Front. Bioeng. Biotechnol. 8, 878. https://doi.org/10.3389/fbioe.2020.00878.
Robin, J., Kerr Graham, H., Selber, P., Dobson, F., Smith, K., Baker, R., 2008. Proximal femoral geometry in cerebral palsy: a population-based cross-sectional study. J. Bone Jt. Surg. - Ser. B 90, 1372–1379. https://doi.org/10.1302/0301-620X.90B10.20733.
Rodda, J., Graham, H.K., 2001. Classification of gait patterns in spastic hemiplegia and spastic diplegia: a basis for a management algorithm. Eur. J. Neurol. 8 (Suppl. 5), 98–108.
Sangeux, M., 2019. Biomechanics of the Hip During Gait. In: The Pediatric and Adolescent Hip. Springer International Publishing, pp. 53–71. https://doi.org/10.1007/978-3-030-12003-0_3.
Schwartz, M.H., Rozumalski, A., Trost, J.P., 2008. The effect of walking speed on the gait of typically developing children. J. Biomech. 41, 1639–1650. https://doi.org/10.1016/j.jbiomech.2008.03.015.
Shefelbine, S.J., Carter, D.R., 2004. Mechanobiological predictions of femoral anteversion in cerebral palsy. Ann. Biomed. Eng. 32, 297–305. https://doi.org/10.1023/B:ABME.0000012750.73170.ba.
Steele, K.M., DeMers, M.S., Schwartz, M.H., Delp, S.L., 2012. Compressive tibiofemoral force during crouch gait. Gait Posture 35, 556–560. https://doi.org/10.1016/J.GAITPOST.2011.11.023.
Tayton, E., 2007. Femoral anteversion. J. Bone Joint Surg. (Br.) 89-B, 1283–1288. https://doi.org/10.1302/0301-620X.89B10.19435.
Van Rossom, S., Kainz, H., Wesseling, M., Papageorgiou, E., De Groote, F., Van Campenhout, A., Molenaers, G., Desloovere, K., Jonkers, I., 2020. Single-event multilevel surgery, but not botulinum toxin injections normalize joint loading in cerebral palsy patients. Clin. Biomech. (Bristol, Avon) 76, 105025. https://doi.org/10.1016/j.clinbiomech.2020.105025.
Veerkamp, K., Schallig, W., Harlaar, J., Pizzolato, C., Carty, C.P., Lloyd, D.G., van der Krogt, M.M., 2019. The effects of electromyography-assisted modelling in estimating musculotendon forces during gait in children with cerebral palsy. J. Biomech. https://doi.org/10.1016/J.JBIOMECH.2019.05.026.
Viceconti, M., Olsen, S., Nolte, L.P., Burton, K., 2005. Extracting clinically relevant data from finite element simulations. Clin. Biomech. https://doi.org/10.1016/j.clinbiomech.2005.01.010.
Wesseling, M., Kainz, H., Hoekstra, T., Van Rossom, S., Desloovere, K., De Groote, F., Jonkers, I., 2020. Botulinum toxin injections minimally affect modelled muscle forces during gait in children with cerebral palsy. Gait Posture 82, 54–60. https://doi.org/10.1016/j.gaitpost.2020.08.122.
Wren, T.A.L., Rethlefsen, S., Kay, R.M., 2005. Prevalence of specific gait abnormalities in children with cerebral palsy: influence of cerebral palsy subtype, age, and previous surgery. J. Pediatr. Orthop. 25, 79–83.
Yadav, P., Shefelbine, S.J., Gutierrez-Farewik, E.M., 2016. Effect of growth plate geometry and growth direction on prediction of proximal femoral morphology. J. Biomech. 49, 1613–1619. https://doi.org/10.1016/j.jbiomech.2016.03.039.
Yadav, P., Shefelbine, S.J., Pontén, E., Gutierrez-Farewik, E.M., 2017. Influence of muscle groups' activation on proximal femoral growth tendency. Biomech. Model. Mechanobiol. 16, 1869–1883. https://doi.org/10.1007/s10237-017-0925-3.